UNIVERSITÀ DEGLI STUDI FIRENZE
DIEF DIPARTIMENTO DI INGEGNERIA INDUSTRIALE

ADDITIVE 4 BIOMEDICAL

October 17th–18th, 2022

IMPROVED BIOMECHANICAL BEHAVIOR OF 316L GRADED SCAFFOLDS FOR BONE TISSUE REGENERATION PRODUCED BY LASER POWDER BED FUSION

Maria Laura Gatto

Dept. DIISM, Univpm, Ancona, Italy
m.l.gatto@staff.univpm.it

Plesso Didattico Morgagni, Viale Morgagni, 44-48, 50134 Firenze

SC 09/A3 CoCo AM Additive Manufacturing

ASSOCIAZIONE NAZIONALE DISEGNO E METODI

COMET

aias

BACKGROUND

- **316L SS** is a cost-effective solution for short-term bone implants
- Scaffold for bone regeneration should possess porous network allowing **mass transport**
- Scaffold **mechanical properties** are required to match with tissue, to prevent stress shielding effect
- **Graded lattice geometry** is a potential solution to meet biomechanical needs, providing adaptative porous gradient
- Functional grading also allows **designing deformation behavior** of the scaffold, by controlling the local relative density of unit cells
- **LPBF** allows to achieve high accuracy of internal architecture, also in case of intricate pattern and micro-scaled reticula

STATE OF ART

- Until now, studies on 316L SS scaffolds produced by LPBF technology were limited to **gyroid**, **lattice** and **topology-optimized lattice** geometries [T. Zhong 2019; J. Čapek 2016; M. Fousová 2017, Z. Xiao 2018, X. Cao 2018].

- The only study on optimization of a 316L SS LPBF graded lattice scaffold, for programming its plastic deformation behavior, is **not applied to biomedical** implants [O. Al-Ketan 2021].

AIM

Graded lattice geometries were produced in 316L by LPBF technology for designing the biomechanical behavior of scaffold

MATERIALS AND METHODS

- **Geometry**: Dense-in (DI) and dense-out (DO) graded lattice scaffold geometries

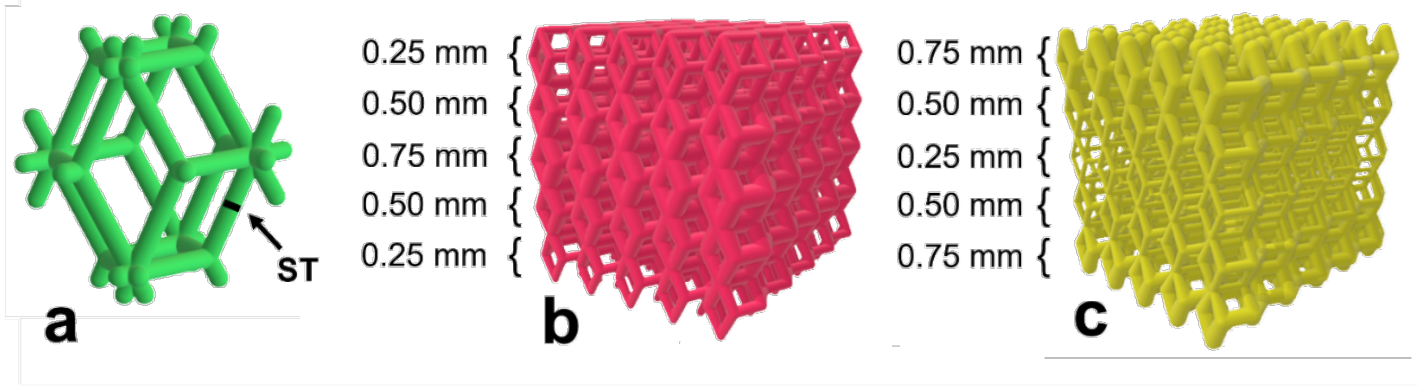

- **Biomaterial**: Raw powder of 316L SS from LPV CARPENTER Technology

- **Production process**:
  - LPBF using 3D4steel manufacturing system (3D4Mec Srl, Sasso Marconi, Italy)
  - 300 W Yb-fiber laser
  - Nitrogen atmosphere

Parameter	Range
Laser power [W]	200 - 270
Scan speed [mm/s]	400 - 1000
Hatching distance [mm]	0.10 - 0.14
Thickness [mm]	0.02 - 0.06

MATERIALS AND METHODS

- **Experimental porosity**:

$$P_{EXP} = \frac{(V_S - V_{mEXP})}{Vs} * 100$$

- V_s = 1000 mm^3
- m_{DI} = 3.67 ± 0.04 g
- m_{DO} = 2.41 ± 0.05 g
- ρ_{mat} = 7.9 g/cm^3 [A. Röttger, 2020]

- **Relative density**:

$$\rho = 1 - \frac{P_{EXP}}{100}$$

- **SEM & EDS**: Tescan VEGA3 scanning electron microscope equipped with EDAX Elements microanalysis

- **XRD**: Bruker D8 Advance diffractometer operating at V = 40 kV and I = 40 mA, with Cu-Kα radiation

MATERIALS AND METHODS

- **Pattern analysis**: DIFFRAC.EVA (Bruker AXS) software by using the PDF2 database of the International Centre for Diffraction Data (ICDD).
- **Rietveld refinement**: MAUD software (Material Analysis Using Diffraction)
- **Peak shape analysis**: OriginPro (Vers. 2022. OriginLab Corporation, Northampton, MA, USA) software.

Average crystallite size by the Scherrer formula:

$$L = \frac{K\,\lambda}{\beta\,cos\theta}$$

- **λ**=0.154056 nm, wavelength of Cu-Kα radiation
- **β** Full Width at Half Maximum (FWHM)
- **θ** Bragg angle (unit: rad)
- **K** a dimensionless number of the order of unity known as the Scherrer constant, which is related to crystallite size [B.D. Cullity, 1956].

MATERIALS AND METHODS

- **XμCT analysis**: Zeiss Metrotom 1500 tomographic system @ V=199 kV, I=130 μA and 0.75 mm Cu filter, with pixel size 11.2 μm

- **Mechanical tests**: INSTRON 5567 machine, with 30 kN load cell at 0.5 mm/min speed, according to ISO 13314:2011

- **Biological tests**:
  - **Sterilization**: Autoclaved + 30 min UV irradiation;
  - **Cells**: MG-63 human osteosarcoma cells;
  - **Viability test**: MTT assay and cellular morphology after 24 h and 7 d from seeding.

RESULTS | EDS

Sample/Element	Cr (wt.%)	Mn (wt.%)	Mo (wt.%)	Ni (wt.%)	Si (wt.%)	Fe
PW	17.7 ± 0.2	1.6 ± 0.2	2.30 ± 0.03	12.0 ± 0.3	0.74 ± 0.05	Bal.
DI	17.7 ± 0.2	2.5 ± 0.4	2.0 ± 0.2	12.1 ± 0.1	1.3 ± 0.4	
DO	18.0 ± 0.5	2.3 ± 0.5	2.1 ± 0.2	11.9 ± 0.2	1.5 ± 0.5	

- Scaffolds show a slight increase of **Mn** and **Si** as compared to powder, due to amorphous Mn-Si-rich spherical nano-precipitates [O. Salman 2019];

- Amounts of **Cr** and **Mo** (ferrite stabilizers) as well as of **Ni** (austenite stabilizer) remain almost the same.

RESULTS | XRD

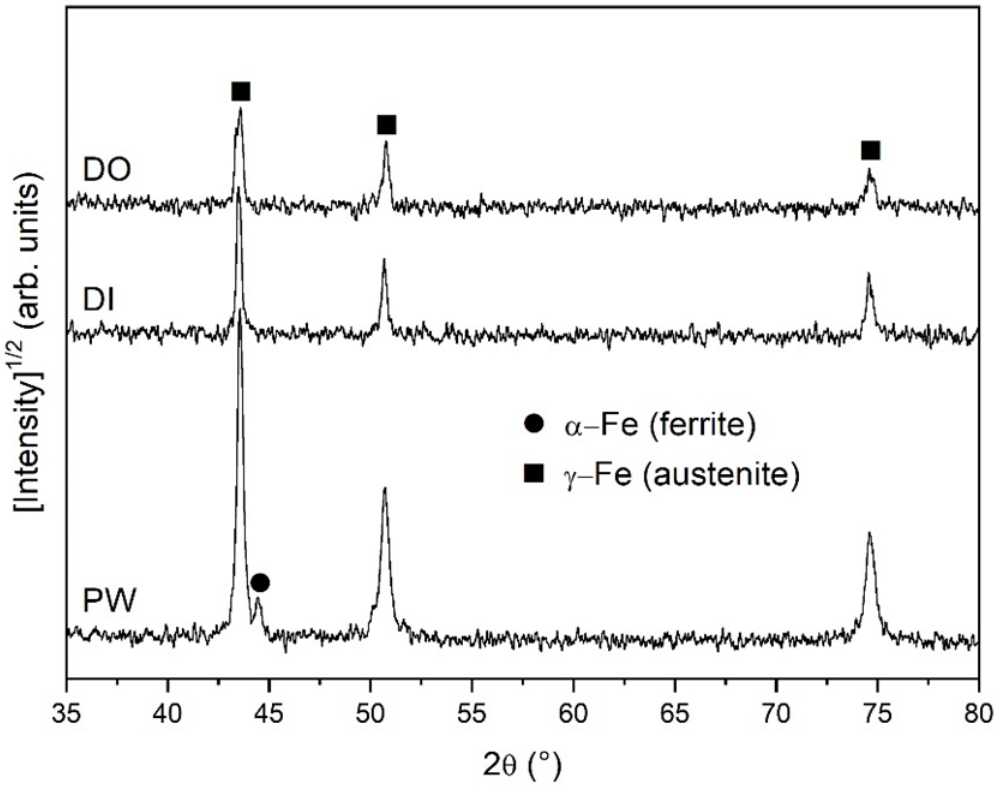

Presence of **α-Fe (ferrite)** in raw powder only, while scaffolds are entirely formed of **γ-Fe (austenite)**, without any crystallographic fibre texture

RESULTS | XRD

Sample	Peak	2θ (°)	FWHM (°)	L (nm)	a_{exp} (nm)	$\Delta a/a_{nom}$ (%)
PW	γ-Fe (111)	43.5525 ± 0.0008	0.178 ± 0.002	47.5 ± 0.5	0.3596 ± 0.0001	0.14
	α-Fe (110)	43.672 ± 0.002	0.30 ± 0.03	28 ± 3	0.2929 ± 0.0002	2.18
DI	γ-Fe (111)	43.4715 ± 0.0008	0.116 ± 0.002	73 ± 1	0.3603 ± 0.0001	0.33
DO	γ-Fe (111)	43.487 ± 0.001	0.113 ± 0.003	75 ± 2	0.3601 ± 0.0001	0.28

- **Scaffolds**: γ-Fe has lattice parameter very close to the nominal one (Δa/anom < 0.4 %), with almost same value of crystallites size (~ 74 nm)
- **Powder**:
  - γ-Fe is formed of smaller crystallites (~ 47 nm) with lattice parameter almost coincident to nominal value;
  - α-Fe is formed of fine crystallites (size ~ 30 nm) with lattice parameter value about 2% higher than the nominal one.

RESULTS | XCT

Source	Parameter	DI	DO
XμCT	Specific surface [mm^{-1}]	11	17
	Closed porosity (P_C) [%]	0.3	0.2
	Open porosity (P_O) [%]	50	71
STL	P_{STL} [%]	58	72
Experimental	P_{EXP} * [%]	55	70
	Relative density (ρ) **	0.45	0.30

- Micro-porosity inside the material is responsible for PC, which in turn determines **material density**;
- Macro pores linked to the elementary **unit cell geometry** constitute PO;
- Discrepancy in DI porosity imputable to real strut size and **residual powder** in scaffold core, due to small open pores and high thermal capacity.

RESULTS | MECHANICAL TEST

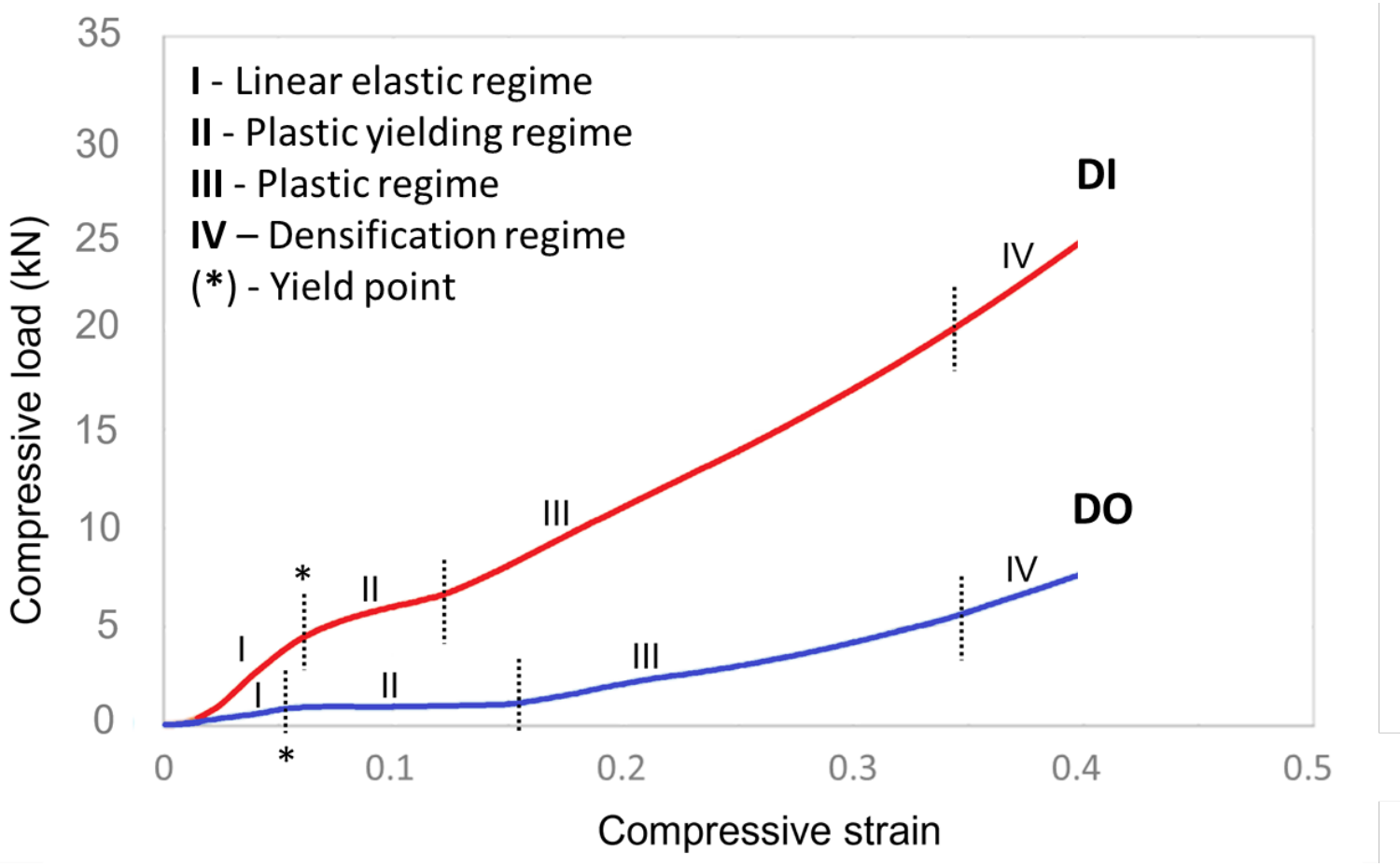

Absence of oscillations and **preferential compaction** of layers with thinner struts → **different deformation mechanism** are simultaneously active during compression

RESULTS | MECHANICAL TEST

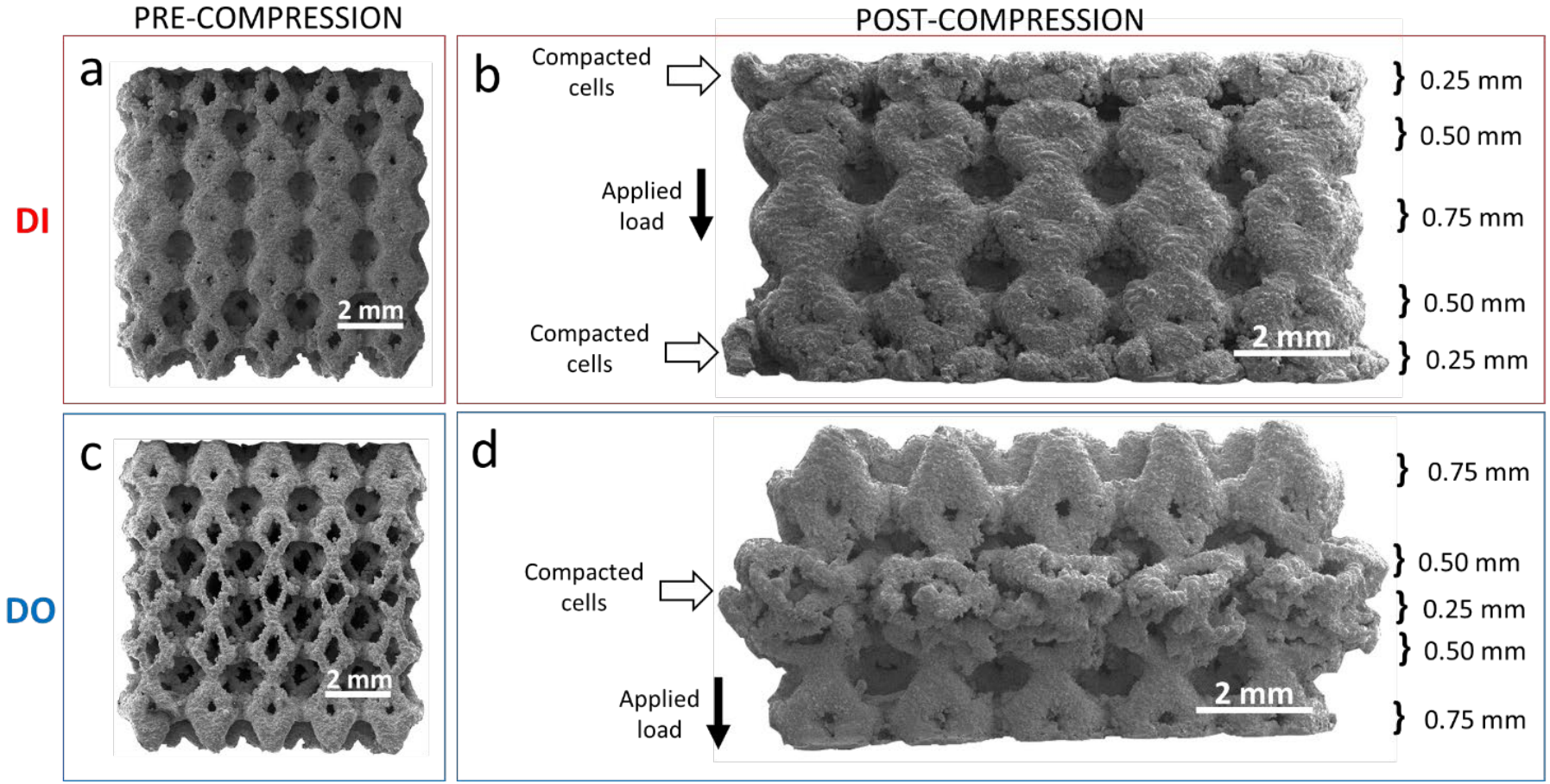

Predominant failure mechanism in graded structures initiates in correspondence of thinner struts, due to high stress concentrations on strut junctions

RESULTS | MECHANICAL TEST

Geometr	σ_{20} [MPa]		σ_{UC} [MPa]		E [MPa]	
y	AV	SD	AV	SD	AV	SD
DI	115	10	255	15	610	90
DO	23	3	80	6	310	100

- Different distribution of strut size in graded geometries is the main factor influencing mechanical response → DI shows **mechanical properties** always higher than DO;

- σUC value for DO is very close to the experimental value of **cortical bone**.

RESULTS | BIOLOGICAL ASSESSMENT

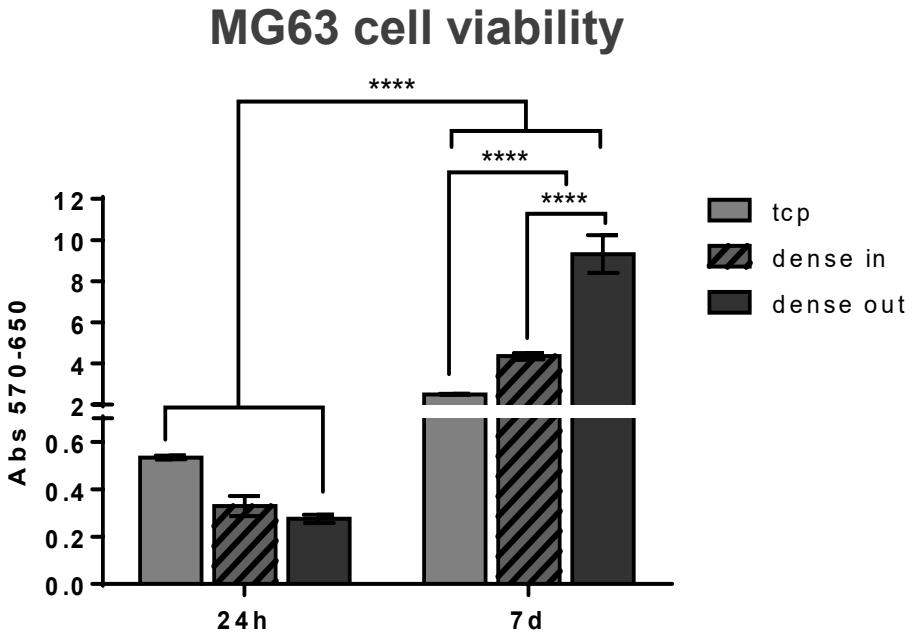

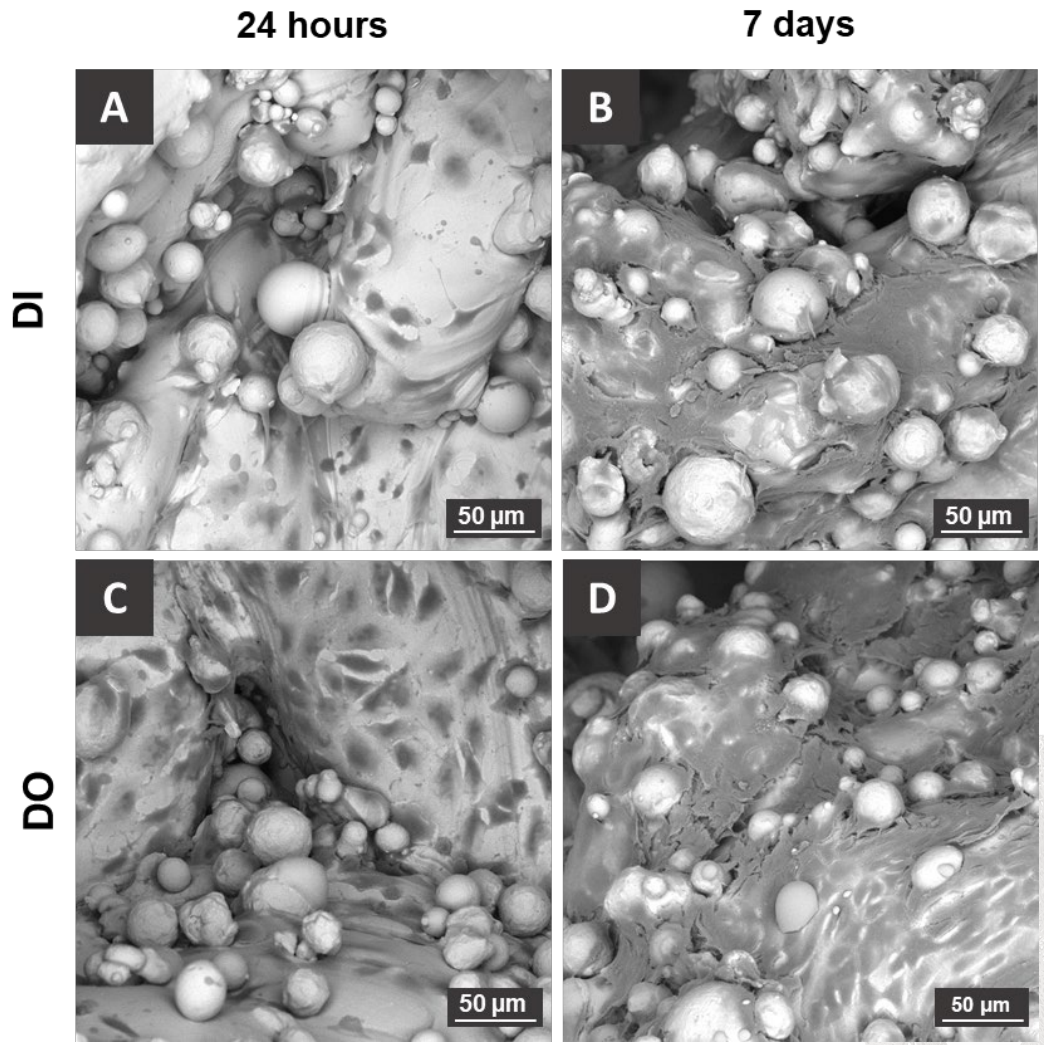

- Highest metabolically active cells on **DO**;
- **Cells spreading** on scaffold surfaces after 24h (A, C);
- Cells start producing **ECM** after 7 days (B, D).

ADDITIVE 4 BIOMEDICAL

CONCLUSIONS

Aim: designing scaffold biomechanical performances for bone tissue regeneration

- DI and DO scaffolds are fully dense (ρ > 99.5%) and fully austenitic with crystallite size of about 75 nm, without any texture developed during the building process;
- Plastic deformation in graded lattices firstly involves struts of smaller size → time sequence of deformation undergoes time shift depending on strut size;
- DO shows mechanical properties close to cortical bone;
- DO improves MG63 cell proliferation as compared to DI.

Improved biomechanical performances of scaffolds can be designed by properly controlling production parameters in the LPBF process and elementary unit cell geometry in graded structures.

UNIVERSITÀ DEGLI STUDI FIRENZE
DIEF DIPARTIMENTO DI INGEGNERIA INDUSTRIALE

October 17th–18th, 2022

THANKS FOR YOUR ATTENTION!

Maria Laura Gatto

Dept. DIISM, Univpm, Ancona, Italy
m.l.gatto@staff.univpm.it

Plesso Didattico Morgagni, Viale Morgagni, 44-48, 50134 Firenze

ADDITIVE 4 BIOMEDICAL

SC 09/A3 CoCo AM Additive Manufacturing

ASSOCIAZIONE NAZIONALE DISEGNO E METODI

COMET

aias